Tight-binding molecular-dynamics study of ferromagnetic clusters

Antonis N. Andriotis
Institute of Electronic Structure and Laser, Foundation for Research and Technology-Hellas, P.O. Box 1527, Heraklio, Crete, Greece 71110

Madhu Menon*
Department of Physics and Astronomy, University of Kentucky, Lexington, Kentucky 40506-0055 and Center for Computational Sciences, University of Kentucky, Lexington, Kentucky 40506-0045

(Received 15 October 1997)

A minimal parameter tight-binding molecular-dynamics scheme incorporating a Hubbard Hamiltonian for the treatment of magnetic effects is detailed. The computational efficiency of the scheme allows applications to cluster sizes well beyond the range of *ab initio* techniques. The method is used to obtain magnetic moments of Ni, Fe, and Co clusters in excellent agreement with experiment. [S0163-1829(98)01416-7]

I. INTRODUCTION

Stern-Gerlach experiments performed on clusters of transition-metal atoms[1–6] (CTMA's) are usually analyzed under the assumption that the CTMA's are single-domain magnetic particles. Depending on the conditions of each experiment, the profiles of the CTMA's being deflected by the Stern-Gerlach magnet exhibit either superparamagnetic or anisotropy-induced relaxation.[7] The latter case occurs when the thermal relaxation time $\tau_{\rm th}$ of the clusters is much larger than their observation time, τ_p, i.e., the time required by the clusters to pass through the poles of the Stern-Gerlach magnet. On the other hand, superparamagnetic behavior is exhibited if the experimental setup allows the condition $\tau_{th} \ll \tau_p$ to be satisfied. According to the theory of superparamagnetism,[8,9] the magnetic moments within a CTMA move coherently, and thus the magnetic moment M_n of a CTMA consisting of n atoms can be represented by a single vector of magnitude equal to

$$M_n = n\langle \mu_n \rangle , \tag{1}$$

where $\langle \mu_n \rangle$ is the average value of the magnetic moment per atom of the cluster.

Recent experimental results[1–6] have confirmed the superparamagnetic behavior of CTMA's in suitably chosen experimental setups. The basic quantity that is measured from these experiments is the average value of the magnetic moment per atom, $\langle \mu_n \rangle$, and its variation with temperature, magnetic field, and size of the cluster. Such data have been recently reported for the clusters Ni_n, Fe_n, and Co_n with $n \leqslant 700$.[2–6] The variation of $\langle \mu_n \rangle$ with the cluster size (i.e., the number of atoms of the cluster, n) has been experimentally obtained at temperatures $T = 78$ K (Ref. 5) and $73 \leqslant T \leqslant 198$ K (Ref. 6) for Ni_n, $T = 120$ K (Ref. 5) for Fe_n, and $T = 78$ K (Ref. 5) for Co_n clusters. From these results one observes that, for small clusters, $\langle \mu_n \rangle$ exhibits values much larger than those corresponding to the bulk materials and that, as n increases, $\langle \mu_n \rangle$ decreases, although not always monotonically, toward its corresponding bulk value, the latter being practically attained for $n \approx 500-700$. Further analysis of the existing experimental findings for the variation of $\langle \mu_n \rangle$ with the cluster size shows sharp dips superimposed on the monotonic decrease of $\langle \mu_n \rangle$ with n for cluster sizes for which closed icosahedral geometries are possible (i.e., for $n = 13,33,55$, etc.)[6] Furthermore, a comparison among the reported experimental data reveals a noticeable spread within relatively large error bars for the measured values of $\langle \mu_n \rangle$, especially in the case of small Ni_n, Fe_n, and Co_n clusters.[5,6] Such a spread may be partially attributed to the different experimental temperatures at which the reported data were obtained.

Although a lot of experimental data have been reported that confirm the superparamagnetic behavior of the CTMA's,[2–6] detailed analysis of experimental data about the dependence of $\langle \mu_n \rangle$ on the cluster size and/or the cluster geometry is limited. This dependence is formally expressed by the relationship

$$\langle \mu_n \rangle = \mu(n, \{\mathbf{R}_n\}), \tag{2}$$

where $\{\mathbf{R}_n\}$ denotes the geometric configuration of the cluster or, alternatively, the set of position vectors of the atoms of the cluster. To the best of our knowledge, the existing experimental information about the relationship described by Eq. (2) is limited, and refers only to the detailed dependence of $\langle \mu_n \rangle$ on the cluster size,[5,6] and no experimental data have been found reporting the dependence of $\langle \mu_n \rangle$ on the cluster configuration $\{\mathbf{R}_n\}$, a case for which only theoretical data are available.[10–32]

The ground state geometry of the CTMA's is usually obtained from a different class of experiments, namely, those utilizing either photoelectron spectroscopy[33–35] or chemical probe methods.[36,37] The chemical probe experiments indicate strong evidence for icosahedral packings of small CTMA's, and this geometry is assigned to the geometry of the free clusters by assuming that the probings do not affect the geometry of the clusters. The icosahedral geometries of the small CTMA's, as well as a growth mechanism which is well explained by the umbrella model of cluster growth, have gained strong support from experimental results using the photoionization spectroscopy.[33,34]

The theoretical studies of CTMA's need to explain not only the experimental findings but also a host of other interesting features. They include the study of how an atomic property evolves into its corresponding bulk feature. An example of this property would be, say, the atomic (local) magnetism. Another interesting feature is the possibility of constructing new materials, relying on a cluster-type building-block, that has recently attracted much technological interest and, in turn, generated theoretical interest as well.

The main challenge to the theoretical study is summarized by Eq. (2), which shows the dependency of $\langle \mu_n \rangle$ on $\{\mathbf{R}_n\}$ for a given value of the number of atoms n of the cluster. The important issue that needs to be addressed is how the geometric ordering of the cluster affects its magnetic ordering, and vice versa. From early investigations,[17,18,38,39] it became clear that the magnetic behavior of the cluster is the result of a very delicate interplay among various factors, such as the symmetry of the cluster, the bond lengths, the coordination numbers, the size of the cluster, and, finally, the chemistry of its constituent atoms. Any one of these factors could play a dominant role in the magnetic behavior of the cluster. As noted by Castro and Salahub,[26] the types of chemical bonds and patterns of charge distribution influencing the $\langle \mu_n \rangle$ values in CTMA's depend on the total spin states. A striking example is the result of Dunlap,[19] who showed that for fcc-Fe_{13}, an increase in the bond length from 4.4 to 4.81 a.u. is accompanied by an increase in M_n from 32 to 44 Bohr magnetons, μ_B. Other examples illustrating this delicate interplay between geometric and magnetic ordering were given by Mlynarski and Salahub,[11] who observed that, for Ni_4 and Ni_5 clusters, a significant decrease in the coordination number increases the splitting between the spin-up and spin-down electrons, thereby enhancing the value of $\langle \mu_n \rangle$. On the other hand, they also noticed that a contraction in the Ni-Ni bond in Ni_4 may result in a reduction of the local magnetic moments due to an increase in the d-band-width. We have also shown[31] that the energies of the various spin states of a CTMA of given size lie very close to each other, and correspond to almost identical geometric configurations.

All these results indicate that, in order for one to properly describe the magnetic behavior of the CTMA's, it is necessary to obtain an accurate estimation of the ground state of the CTMA as a function of the independent parameters mentioned above. This means that accurate total-energy calculations need to be performed for each cluster in order to locate its minimum-energy configuration with respect to a simultaneous variation in all the independent parameters (on which the total energy depends). Additionally, it must be kept in mind that a profound understanding of the cluster magnetism requires that electron correlation effects be approximated satisfactorily.

It is thus clear that the determination of the ground state of magnetic clusters is a very difficult computational task, which, at the *ab initio* level, becomes formidable, even for clusters of intermediate sizes, i.e., for $10<n<100$. So far, most of the calculations on CTMA's have been performed within the local-electron-spin-density approximation, (LSDA), because the size and the complexity of the transition-metal atoms do not allow a configuration-interaction (CI) approach to CTMA's. The CI calculations are usually restricted only to monomers and/or dimers, and very often the accuracy of the CI calculation achieved is crucial in the ground-state determination of a transition metal-atom and/or a dimer. In Ref. 29, we give a summary of various methods used and results obtained from applications on Ni_n clusters. On the other hand, due to the formidable computational requirements, the LSDA-based *ab initio* calculations, which include a global symmetry unconstrained geometry-relaxation and an unrestricted total spin value for the cluster, are very rare and are usually restricted to cluster sizes with $n \leqslant 10$. For larger clusters, the common practice is to allow the variation of only a limited number of the independent parameters of the system while performing a restricted (constrained) minimization of the total energy of the cluster in order to determine its ground state. The most commonly employed calculational restrictions include one or more of the following approximations: (i) A global-symmetry-constrained geometry relaxation, which allows only a variation in the bond length while keeping the symmetry of the cluster fixed. (ii) A limited symmetry variation keeping the bond lengths fixed (the latter usually kept at their bulk values). (iii) Suppression of some Hamiltonian interactions [e.g., neglect of the s-d interactions in a tight-binding (TB) description]. (iv) Restriction of the total spin value (or equivalently the value of M_n) during geometry optimization. [In such an approximation, M_n is not allowed to take any dependence on the cluster configuration $\{\mathbf{R}_n\}$ during a molecular dynamics (MD) relaxation process. Instead, several MD processes are repeated, keeping a different value of M_n each time. Unless many such processes of various fixed M_n value are carried out, the spin-restricted results will not be accurate considering the large number of closely spaced local-energy minima resulting from the $\{\mathbf{R}_n\}$ dependence]. (v) Electron correlations are usually treated within the LSDA and/or Hubbard model approximation.

The above list of approximations also includes various model approximations,. They include, for example, the popular spherical jellium-drop model and its modifications,[41–46] which have been found to be successful in describing various properties of clusters of simple metals. In the case of CTMA's, however, the models based on the jellium approximation are inadequate to describe the cluster magnetism and/or its effect on the cluster geometry. Even the reintroduction of lattice effects within a pseudopotential formalism,[43,44] in a fashion similar to that proposed by Andriotis[47] for the semi-infinite metals, cannot overcome the inherent limitations of the jellium approximation. Furthermore, the conducting spherical jellium-drop model[45,46] has also been found to be inadequate in describing nonmagnetic properties of CTMA's, namely, their ionization energies.[34,40]

Faced with these difficulties, the theoretical efforts have been led to a search for workable simpler computational schemes in order to describe both small and large CTMA's at the same level of accuracy. Among the models proposed, those which combine MD schemes with the embedded-atom many-body potential methods[20,48–50] were found to be reasonably successful in determining the structural properties of nonmagnetic CTMA's. Similarly, methods based on empirical model potentials[51,52] have been used for analyzing the structural, dynamical, meltinglike, and evaporation behaviors of transition- and noble-metal clusters (see Ref. 51 and references therein). However, by their nature, these methods

cannot be used for a description of cluster magnetism, except for the embedded potential methods which can be used for an approximate description of the cluster magnetism provided that additional approximate corrections be incorporated into the original scheme of these theories.[20] A better way to describe the cluster magnetism is provided by the tight-binding method, which has been used successfully in a description of the bulk[53,54] and surface magnetism.[55–57] For this reason, and motivated by the success of the tight-binding molecular-dynamics (TBMD) method in the treatment of semiconductor systems,[58] we have recently introduced the TBMD calculational approach in the studies of CTMA's. In a series of recent works,[27–29] we have demonstrated that the TBMD method can be used to successfully describe the structural and dynamical properties of nonmagnetic Ni_n clusters of small and intermediate sizes (i.e., for $n \leqslant 55$). Using the TBMD scheme we were able to show that, in agreement with the experiment, Ni_n clusters, in their ground state, ''prefer'' the icosahedral structure over the fcc ones when the cluster size permits the cluster to form a closed icosahedron (i.e., for $n=13,33,55$, etc.). For all other cluster sizes, however, the fcc-based structures were found to be energetically more favorable than the icosahedral ones.[27–29] Subsequently, by including electron correlations within the Hubbard model approximation in our TBMD approach, we were able to extend our applications to the magnetic Ni_n, Fe_n, and Co_n ($n \leqslant 55$) clusters.[30,31] We also showed in earlier reports[30,31] that our extended TBMD approach—to be referred to as the *H*-TBMD method—leads to a description for the variation of the average magnetic moment $\langle \mu_n \rangle$ per atom with the cluster size in very good agreement with the existing experimental data.[5,6]

In our *H*-TBMD approach, as in our original TBMD, much emphasis is focused on the flexibility and efficiency of the method to allow for spin and symmetry unrestricted total-energy optimizations for CTMA's of small and intermediate sizes within the LSDA. *H*-TBMD imposes no symmetry and spin constraints, while at the same time including all electron-electron interactions within the TB picture and the LSDA without restricting them only among the *d* electrons (as is the case sometimes[16]). As a result, within our *H*-TBMD method, one avoids all the drawbacks associated with any neglect of the *s*-*d* interactions (which seem to reduce $\langle \mu_n \rangle$ by 10% in small iron clusters,[59] and could possibly affect the geometry of the nickel clusters[16]). Additionally, one can study changes in the electron populations that take place among the electron subbands as the total spin and the geometry of the cluster change during the MD simulations.

It is worth emphasizing that the TB method meets a more general acceptance in studies of CTMA's, and many applications have been reported at various levels of approximation.[16,20,21,28–31,59–61] corresponding mostly to the various ways that one can achieve the optimum transferability of the TB parameters. The transferability of the TB Hamiltonian depends on, among other factors, the scaling of the matrix elements with the interatomic distance (see, for example, Ref. 62 and references therein) as well as the scaling factors that take into account the effects of the local environment of each atom.[61,63] In the case of the *H*-TBMD method, the accuracy of the TB approximation also depends on the proper description of the electron correlations within the Hubbard model. This, in turn, is reflected in the choice of the Hubbard parameters for the intrasite and intersite Coulomb and exchange interactions, and also on the degree of self-consistency which is required for their description.[16,20,21,30,31,59–61,64,65]

Our method is very general, and can be applied at various levels of approximations depending on the accuracy desired and the availability of computer resources. The results presented in this work have been performed within the simplest possible approximation. In particular, we have retained the universal TB description of the electronic interactions as proposed by Harrison,[66] using the Slater-Koster [67] scheme, and have included electron correlations within the Hubbard model approximation. Finally, our total-energy expression for the cluster also includes a pair repulsive potential term, suitably fitted to experimental (or *ab initio*) data. These approximations are consistent with our initial motivation to present an efficient methodology based on a minimal set of adjustable parameters (in our case there are only five such parameters), and flexible enough to accurately reproduce known properties when applied to both covalent and metallic systems. On the other hand, the *H*-TBMD method can easily incorporate more accurate TB scaling schemes, as for example the one proposed by Mehl and Papaconstantopoulos,[68] which will allow our method to take a firm *ab initio* character.

II. METHOD

Our TBMD method was described in detail in Ref. 29. In the present work, we focus on the generalization of the TBMD method, namely, the *H*-TBMD method, which was recently introduced in the studies of the magnetic CTMA's.[30,31] A number of minor modifications in the parameters, including the scaling, have been deemed necessary for better transferability of the TB parameters. Whenever necessary, a brief review of the aspects of the original TBMD theory will be given for reasons of completeness. As in our original TBMD approach, the *H*-TBMD method involves the following computational steps.

(i) Construction of the spin unrestricted TB Hamiltonian, $H_\sigma, \sigma = \pm 1$, for electrons with spin-up ($\sigma = +1$) and spin-down ($\sigma = -1$), respectively, from which the electronic eigenstates, $|c_{i\sigma}\rangle$, and eigenvalues, $\epsilon_{i\sigma}$, are calculated (within the LSDA) by solving the Schrödinger equation

$$H_\sigma |c_{i\sigma}\rangle = \epsilon_{i\sigma} |c_{i\sigma}\rangle. \tag{3}$$

(ii) Calculation of the total-energy of the system by summing over occupied levels and adding a sum over pair potentials. The total-energy expression is then used in the calculation of forces acting on each atom of the system.

(iii) Full geometry optimization of the system by following its time evolution starting from specific initial geometries.

A. Construction of the spin-unrestricted TB Hamiltonian

In constructing the TB Hamiltonian, we assume an orthogonal atomic basis set. For the case of nonmagnetic CTMA's the diagonal Hamiltonian (i.e., the intrasite) matrix

elements $E_m^{(i)}, m=s,d$, associated with the atom at the lattice site $\mathbf{R}_i$, are taken to be configuration independent and equal to the values given by Harrison.[66] Note that p orbitals are not used here, and we take $E_s^{(i)}=E_d^{(i)}$. For the latter approximation, Harrison readjusted the value of the intersite matrix element $V_{ss\sigma}$ in order to fit the bulk band structure. It is clear that Harrison's diagonal elements cannot be directly used for studying cluster properties which depend explicitly on the relative strength and position of the atomic orbital energies.

In the case of the magnetic CTMA's, the necessary spin dependence of the diagonal matrix elements is introduced using the Hubbard approximation according to which[69] the intra-atomic Coulomb and exchange interactions result (in the case of atoms with band degeneracy) in an effective intra-atomic Coulomb repulsion $U_{\rm eff}^{(i)}$ and a corresponding effective intra-atomic exchange interaction $J_{\rm eff}^{(i)}$, in terms of which the corrections $\Delta E_m^{(i)}, m=s,d$, to the diagonal elements $E_m^{(i)}, m=s,d$ take the form

$$\Delta E_{m\sigma}^{(i)}=U_{\rm eff}^{(i)}\Delta n_{m\sigma}^{(i)}-\sigma\mu_m^{(i)}J_{\rm eff}^{(i)}+\Delta E_{\rm Mad}^{(i)}+\Delta E_{\rm config}^{(i)}, \quad m=s,d \tag{4}$$

where σ denotes the spin ($+1$ for spin-up and -1 for spin-down), $n_{m\sigma}^{(i)}$ denotes the occupation number of the $|m\sigma\rangle$ orbital at the lattice site $\mathbf{R}_i$ and

$$\mu_m^{(i)}=n_{m\sigma}^{(i)}-n_{m-\sigma}^{(i)}, \quad \Delta n_{m\sigma}^{(i)}=n_{m\sigma}^{(i)}-n_{0m\sigma}^{(i)}, \tag{5}$$

where $n_{0m\sigma}^{(i)}$ are the corresponding orbital occupancies for the bulk material. The terms $\Delta E_{\rm Mad}^{(i)}$ and $\Delta E_{\rm config}^{(i)}$ contained in the right-hand side of Eq. (4) denote the Madelung-type interactions (resulting from the charge transfer among the atoms of the cluster) and the coordination dependence of the matrix elements, respectively.[56,59–61,64]

The off-diagonal (i.e., the intersite) matrix elements are taken within the two-center approximation of Slater and Koster[67] and scaled exponentially with respect to the interatomic distance r,

$$V_{\lambda\lambda'\mu}(r)=V_{\lambda\lambda'\mu}(d)\exp[-\alpha(r-d)], \tag{6}$$

where d is the equilibrium bond length in the corresponding bulk material, and α is an adjustable parameter in the theory. We use a smooth Fermi-type function to cutoff interactions between atoms separated by large distances, ensuring that the average cutoff distance r_c (≈ 3.00 Å) is between the nearest and next-nearest neighbors in the bulk solid. For the present calculations we follow our previous calculational scheme,[27–29] and assume that the values of the parameters $V_{\lambda\lambda'\mu}(d)$ can be expressed in terms of the universal constants $\eta_{\lambda\lambda'\mu}$ of Ref. 66,

$$V_{\lambda\lambda'\mu}(d)=\eta_{\lambda\lambda'\mu}\frac{\hbar r_d^{\tau}}{md^{2+\tau}}, \tag{7}$$

where r_d is a characteristic length associated with each transition-metal atom.[66] The parameter $\tau=0$ for s-s interactions, $\tau=\frac{3}{2}$ for s-d interactions, and $\tau=3$ for d-d interactions. In Table I we list the values of the universal constants $\eta_{\lambda\lambda'\mu}$ with the exception of $\eta_{ss\sigma}$, which is now an adjustable parameter, and in Table II we list various elements used in the present calculations.

TABLE I. Universal constants (values taken from the solid state table of Ref. 66) used in Eq. (7) for obtaining the interaction parameters in the present work.

Parameter	Value
$\eta_{sp\sigma}$	1.84
$\eta_{pp\sigma}$	3.24
$\eta_{pp\pi}$	−0.81
$\eta_{sd\sigma}$	−3.16
$\eta_{pd\sigma}$	−2.95
$\eta_{pd\pi}$	1.36
$\eta_{dd\sigma}$	−16.20
$\eta_{dd\pi}$	8.75
$\eta_{dd\delta}$	0.00

While our assumption that the intra-atomic (diagonal) TB matrix elements are configuration independent can be justified from the fact that for large CTMA's (i.e., for the systems for which the present H-TBMD method is being formulated), the cluster stability is mainly an interplay between two mutually competing close-packed structures. However, it should be emphasized that in CTMA's of small size, charge transfer and anisotropy effects may induce significant corrections in the diagonal TB matrix elements, making a self-consistent approach necessary in their determination. Furthermore, self consistency may also be necessary for an accurate incorporation of the electron correlation effects in order to obtain a reliable description of the cluster magnetism. In the Hubbard model approximation of the electron correlations, this requirement translates into a boundary condition that imposes self consistency on the occupation numbers of the electron orbitals. The exponential scaling of the interatomic (off-diagonal) TB matrix elements, on the other hand, employed in the present work, can be justified from our experience on Si clusters.[62]

In our H-TBMD approach, we make the simplest possible approximation to the correction terms, $\Delta E_{m\sigma}^{(i)}$, and take

$$\Delta E_{m\sigma}^{(i)}=-\sigma s_{0m}^{(i)}, \tag{8}$$

where $s_{0m}^{(i)}$ are adjustable parameters, to be adjusted so as to reproduce the correct spacing of the higher-spin states of small clusters (for cluster size $n\leqslant 5$), whose values are available from results of accurate *ab initio* calculations. From Eqs. (4) and (8), it is apparent that the parameters $s_{0m}^{(i)}$ correspond to effective exchange interaction $J_{\rm eff}^{(i)}$ terms according to the relation

$$s_{0m}^{(i)}=\mu_m^{(i)}J_{\rm eff}^{(i)}. \tag{9}$$

TABLE II. Adjustable parameters used in the present scheme for Ni, Fe, and Co.

Element	$\eta_{ss\sigma}$	α (Å^{-1})	ϕ_0 eV	s_0	a	b
Ni	−0.47	1.04	0.264	0.50	0.5674	−1.2637
Fe	−0.78	0.75	0.349	1.05	0.1748	−4.6613
Co	−0.51	0.80	0.773	0.55	0.6880	−2.1694

TABLE III. *A priori* parameters used in the present scheme for Ni, Fe, and Co. E_s and E_d are diagonal Hamiltonian (i.e., intrasite) matrix elements, and are taken from the solid-state table of Ref. 66. d is the equilibrium bond length in the corresponding bulk material.

Element	$E_s=E_d$ eV	d Å
Ni	−18.96	2.5
Fe	−16.54	2.48
Co	−17.77	2.48

In order to simplify our model further, we assume the effective exchange interaction to depend only on $\langle \mu_n \rangle$ (and not on the individual $\mu_n^{(i)}$ value) and be independent of the types of the orbitals and lattice sites; i.e., we take

$$s_{0m}^{(i)} = s_0, \quad \forall m,i. \tag{10}$$

Thus the present H-TBMD method includes just one extra adjustable parameter s_0, when compared with our original TBMD method.[29]

The approximations made in Eq. (10) are consistent with the inherent approximations of the method and, to a large extent, can be justified based on the results of *ab initio* calculations. In particular, from the early calculations of Yang *et al.*,[38] it was observed that for the d bands, the effective exchange splitting between corresponding majority- and minority-spin levels in a cluster is of the same order of magnitude as those obtained from band theory (see also Ref. 30). The exchange splitting was found[38] to be a very localized property, not very sensitive to cluster size. Equation (10) is also consistent with Harrison's approximation used here, according to which $E_d^{(i)} = E_s^{(i)}$.[66] These, along with the bond length in the bulk solid d, are set *a priori*, and are listed in Table III.

B. Calculation of total energy and atomic forces

The total-energy calculation proceeds along the original TBMD method.[29] Briefly, the procedure is as follows.

The total energy U is written as a sum of three terms:

$$U = U_{\rm el} + U_{\rm rep} + U_{\rm bond}. \tag{11}$$

The electronic part $U_{\rm el}$ is obtained by performing a sum over the eigenvalues $\epsilon_{i\sigma}$ of the occupied one-electron states of the TB Hamiltonian, given by Eq. (3), i.e.,

$$U_{\rm el} = \sum_{i\sigma}^{\rm occ} \epsilon_{i\sigma}\theta_{i\sigma}, \tag{12}$$

where $\theta_{i\sigma}$ is the occupation number of the $|i\sigma\rangle$ state.

The second term in Eq. (11), $U_{\rm rep}$, is a pair repulsive term that includes contributions from the ion-ion interactions and a correction to the double-counting terms included in $U_{\rm el}$, coming either from Coulomb and exchange interactions or the (Hubbard) correlation terms. This term is given by a sum of repulsive pair potentials, ϕ_{ij},

$$U_{\rm rep} = \sum_i \sum_{j>i} \phi_{ij}(r_{ij}). \tag{13}$$

ϕ_{ij} is taken to scale exponentially with the interatomic distance r_{ij}:

$$\phi_{ij}(r_{ij}) = \phi_0 \exp[-4\alpha(r_{ij}-d)]. \tag{14}$$

The value of ϕ_0 is chosen so as to reproduce the correct experimental bond length of the dimer at its correct magnetic state.[30] In Table II we list our adjusted values for both s_0 and ϕ_0 for Ni, Fe, and Co clusters. The cutoff distance, r_c, used for the repulsive potential, is taken to be the same as that for the electronic term.

The third term $U_{\rm bond}$ is a coordination-dependent correction term to the total energy, originally introduced by Tomanek and Schluter[70] in their studies of Si clusters. Although in our earlier works we used a quadratic polynomial for fitting $U_{\rm bond}$, we find that a linear polynomial is adequate in our improved scheme. This term does not participate in the calculation of the forces and, therefore, does not affect the MD procedure for geometry optimization. It is, however, very crucial in distinguishing various isomers for a given cluster size. Assuming no appreciable dependence on bond length, the $U_{\rm bond}$ term is given by the following expression:

$$U_{\rm bond} = n\left[a\left(\frac{n_b}{n}\right) + b\right], \tag{15}$$

where n_b/n is the average number of bonds per atom of the cluster, and n is the number of atoms in the cluster. The value of n_b is determined by a Fermi-type function, i.e.,

$$\frac{n_b}{n} = \frac{1}{2n}\sum_{i,j}\left[\exp\left(\frac{r_{ij}-r_c}{\Delta}\right)+1\right]^{-1}, \tag{16}$$

where the sum is over all bonds of the cluster and Δ is taken equal to 0.01 Å. The parameters a and b are obtained by fitting $U_{\rm bond}$, given by Eq. (15), to either *ab initio* results for the total energy, $U_{\rm ab\ initio}$, of small clusters of different sizes in their ground state (if available), or experimental results according to the equation

$$U_{\rm bond} = U_{\rm ab\ initio} - U_{\rm el} - U_{\rm rep}. \tag{17}$$

Thus there are a total of five adjustable parameters in our scheme: a and b from Eq. (15), ϕ_0 for the repulsive potential, s_0 for the average exchange splitting, and α for the scaling of both the electronic Hamiltonian and the repulsive potential with the interatomic distance according to Eqs. (6) and (14). These parameters, once adjusted to reproduce known results (theoretical or experimental) for small clusters (with number of atoms less than or equal to 5), are then kept fixed in subsequent calculations for clusters of arbitrary sizes. In Table II we give our fitted values for these parameters.

The force $\mathbf{f}_i$ acting on the ith atom due to the interatomic interactions are obtained from the equation

$$\mathbf{f}_i = -\nabla_i(U_{\rm el} + U_{\rm rep}). \tag{18}$$

The simple analytic form of $U_{\rm rep}$ [Eq. (14)] makes the evaluation of the corresponding force term rather straightforward. The contribution to the force $\mathbf{f}_i$ from $U_{\rm el}$ is obtained by using the Hellmann-Feynman theorem, according to which

$$\nabla_i \epsilon_{k\sigma} = \langle c_{k\sigma}|\nabla_i H_\sigma|c_{k\sigma}\rangle. \tag{19}$$

The spatial derivative of the Hamiltonian appearing in Eq. (19) is obtained by taking the spatial derivative of the Hamiltonian matrix elements parametrized according to Eq. (6). The advantages of the exponential scaling scheme over other schemes in facilitating the evaluation of analytic derivatives should be obvious.

Molecular dynamics can subsequently be performed by numerically solving Newton's equation

$$m\frac{d^2\mathbf{r}_i}{dt^2}=\mathbf{f}_i \tag{20}$$

to obtain the atomic coordinates as a function of time. A small damping force is added to simulate energy loss for reaching the equilibrium configuration for the cluster. Many widely differing initial geometric configurations are considered in the simulations. The final equilibrium configurations thus obtained correspond to local minima of the total energy. Our aim is to identify the cluster configuration corresponding to the absolute minimum of the total energy. For small clusters this is readily achieved. For large clusters, however, we construct initial geometries using clues from experimental or other theoretical works and perform a full symmetry-unrestricted optimization. Although such an approach is considerably efficient, it can still leave out some cluster configurations containing the most stable geometry.

C. Accuracy of the model

The TB parameters are usually obtained by fitting to bulk band-structure results obtained by accurate *ab initio* calculations. As shown by Harrison,[66] the bulk properties are well described by the universal constants $\eta_{\lambda\lambda'\mu}$. Therefore, the only remaining problem with the choice of the TB parameters is their transferability, i.e., their applicability in environments different from the ones used to obtain the TB parameters. This is not always the case, and the TB parameters obtained by fitting to the bulk band structure cannot describe, in general, surfaces and/or clusters in an accurate way. In such cases, transferability can be significantly improved with a judicious choice of the adjustable parameters ϕ_0 and α that enter the force calculations. These are fitted to a dimer for experimental bond length and frequency. This fitting uniquely determines α and ϕ_0, for a given range of s_0 values (see below). Although a small dependence on the cutoff distance r_c is observed, no appreciable change in results is detected if r_c is taken within the range determined by first- and second-nearest-neighbor distances. Larger r_c values are not consistent with the implicit assumption that the universal TB parameters are obtained by keeping only first-nearest-neighbor interactions. It is worth emphasizing that the procedure followed here is different from the one followed in our earlier calculations,[27–31] in which the value of α was taken equal to $2/d$, where d is the equilibrium bond length of the bulk material. The current approach is an improvement over the previous one, as it allows for better transferability by an accurate description of the two extreme structures, namely, the bulk and the dimer, and, therefore, a better interpolation for structures in between. It must be remembered that distance dependence of the TB parameters implicitly contains the effect of the local environment.[63]

It is also desirable to choose a simple analytical expression for the scaling in order to be efficiently used in large-scale computations. This is just the case when Harrison's[66] universal TB parameters for the intersite interactions are scaled with the interatomic distance according to Eq. (6). Bulk properties are found to be well described by this simple scaling.[62] Additionally, the scaling of the intrasite (diagonal) TB matrix elements requires, in general, a more careful treatment as discussed earlier, and with consideration of terms in Eq. (4).

The parameter s_0 is chosen from a range of values that do not alter the fitting result of α and ϕ_0 and, in addition, reproduces the higher-spin states of small clusters. As expected, we find that s_0 depends on α; the larger the value of α, the larger the value of s_0 that is needed to reproduce the magnetic states of small clusters. Under a constant value of α, small changes in s_0 do not alter the results appreciably.[30] Usually, s_0 is chosen within a range of values that satisfy our result found by fitting α and ϕ_0. We find that changing the values of s_0 by up to 5–10 % do not change results appreciably. This is shown in Table IV, where we present our results for small Ni clusters for two fitted values of s_0, (and similarly in Table 1 of Ref. 30 for Fe_n). From these results one observes that the geometries of the various spin states of the Ni (and Fe) clusters are quite stable within fairly large uncertainties of the s_0 value, the latter being very close to the average value of the exchange splitting as obtained from band-structure calculations;[16,17,26,53] (see also Table VI). It is also worth noting that small changes in s_0 (while keeping all the other parameters constant) do not result in any changes in the vibrational frequencies.

The other two parameters, namely, the coefficients a and b which are used to express $U_{\rm bond}$ in Eq. (15), are obtained by fitting $U_{\rm bond}$ values, defined by Eq. (17), to a linear polynomial in the number of bonds per atom (n_b/n) according to Eq. (15). The major problem encountered in the evaluation of the coefficients a and b is the lack of sufficient *ab initio* data for fully optimized (symmetry unrestricted) structures. The situation is exacerbated by the fact that *ab initio* results for cluster geometries, frequencies, and magnetic states fail to agree among themselves and also with experiment, even for small clusters. Since the coefficients a and b require only two sets of data, we chose to use experimental data for the binding energies of the dimer and bulk solid for their determination. As will be shown in Sec. III, this choice leads to good agreement with *ab initio* results when data for fully optimized structures are available. In some cases when experimental results are available for some ''magic number'' clusters, the results obtained using the present scheme seem to give better agreement with experiment than *ab initio* values reported, suggesting that symmetry unconstrained optimization might be more relevant than other factors considered for these clusters.

III. RESULTS

In this section we present our results for Ni_n, Fe_n, and Co_n clusters obtained using the *H*-TBMD scheme.

TABLE IV. Results for Ni_n clusters obtained for two different values of the parameter s_0. (*) Relative to the energy of the lowest energy state (otherwise the $\mu=0$ state has the same energy for different s_o values.) (**) The calculations of Ref. 11 for Ni_4 refer to the T_d geometry.

Cluster	Symmetry	μ	Total energy/atom (eV) Present work $s_o=0.45$	Present work $s_o=0.50$	Ref. 11 LDA	Ref. 11 NL	r_e (Å) Present work	Ref. 11 LDA	Ref. 11 NL
		0	0.450	0.500			2.20		
Ni_2		2	0.000	0.000	0.000	0.000	2.20	2.20	2.03
	C_{3v}	0	0.156	0.189			2.28		
Ni_3	C_{2v}	2	0.000	0.000			2.31×2,2.29		
	C_{2v}	4	0.071	0.038			2.41×2,2.28		
	square	0	0.468(*)	0.518(*)	0.165(**)	0.083	2.27×4,3.16×2	2.49	
	T_d	2	0.032	0.057	0.068	0.020	2.31×2,2.41×4	2.49	
Ni_4	T_d	4	0.000	0.000	0.000	0.000	2.35×3,2.46×3	2.49	2.36
	T_d	6	0.066	0.041	0.163	0.156	2.31,2.48×4,2.49	2.49	
	Trig-Pyr	0	0.249(*)	0.298(*)			2.27–2.84		
	C_{4v}		0.375	0.423	0.260		2.28×4,2.27,2.77	2.49	
	Trig-Pyr	2	0.241	0.269			2.32×6		
	C_{4v}		0.166	0.195			2.31–2.35		
	Trig-Pyr	4	0.000	0.009			2.36–2.91		
Ni_5	C_{4v}		0.054	0.063	0.044			2.49	
	Trig-Pyr	6	0.055	0.043			2.40–2.52		
	C_{4v}		0.080	0.101	0.000			2.49	
	Trig-Pyr	8	0.031	0.000			2.44×4,2.47×4,2.56		
	C_{4v}		0.135	0.164	0.088			2.49	
Ni_6	D_{4h}	6	0.000	0.000			2.33–2.51		
	(distort)	8	0.083	0.067			2.38–2.50		
		10	0.074	0.041			2.41–2.59		
		12	0.097	0.047			2.53×12		

A. Ni clusters

The parameters α and ϕ_0 were chosen to reproduce the experimental bond length (2.20 Å) (Ref. 23) and vibrational frequency (330 cm^{-1}) (Refs. 23 and 71) of the dimer. The bulk bond length obtained using the same parameters is 2.60 Å, which compares favorably with the experimental value of 2.49 Å. The value for s_0 was chosen so as to reproduce the energy spacing of the lower-spin states of small clusters as found by *ab initio* methods.[11] The best fit was obtained by choosing $s_0=0.5$ eV, although small variations in the value of s_0 do not change the results appreciably (as apparent from the results in Table IV). Finally, the values for a and b were obtained by fitting $U_{\rm bond}$ in Eq. (15) to the experimental values of the cohesive energy of the bulk [4.44 eV/atom (Ref. 72)] and the experimental binding energy of the dimer (0.933 eV/atom, the value quoted in Ref. 23; a more recent report[71] gives the value of 1.04 eV/atom). We used the cohesive energy of a relaxed 147-atom cluster to obtain an approximate figure for the bulk value. This fit reproduces fairly well the *ab initio* results of Ref. 32, which, as it is worth pointing out, indicate a noticeable dependence on the bond length. The adjustable parameters used for Ni are listed in Table II. Also listed in the same table are the adjustable parameters used for Fe and Co.

We have considered Ni_n clusters of arbitrary sizes. Although several of our results for the magnetic Ni clusters have been published recently,[30,31] we recalculate many of the structures using the currrent parametrization scheme. In particular, we focus on cluster sizes most studied using other theoretical methods for purposes of comparison.

As will be shown below, the current parametrization does not introduce qualitative differences in our results when these are compared with those obtained with our earlier parametrization.[27–31] Only small quantitative differences are introduced by the current parametrization, and these pertain mainly to the energetics of the various cluster structures. Thus, within the current parametrization, we find that, in agreement with our previous parametrization,[31] the magnetic Ni_{13} cluster does not exhibit a stable icosahedral ground state; instead, initial icosahedral geometries relax to a very distorted geometry of a prismlike structure, which is only 0.020 eV/atom less stable than the one obtained by relaxing fcc structures. For Ni_{19}, we find that the nonmagnetic icosahedral cluster is less stable than the corresponding fcc one by 0.135 eV/atom. For the magnetic Ni_{19}, the fcc structure (with $\langle\mu_n\rangle=0.842\mu_B$) is found to be more stable than the icosahedral one (with $\langle\mu_n\rangle=1.158\mu_B$) by 0.013 eV/atom. Similarly, we find that the magnetic (nonmagnetic) fcc Ni_{43}

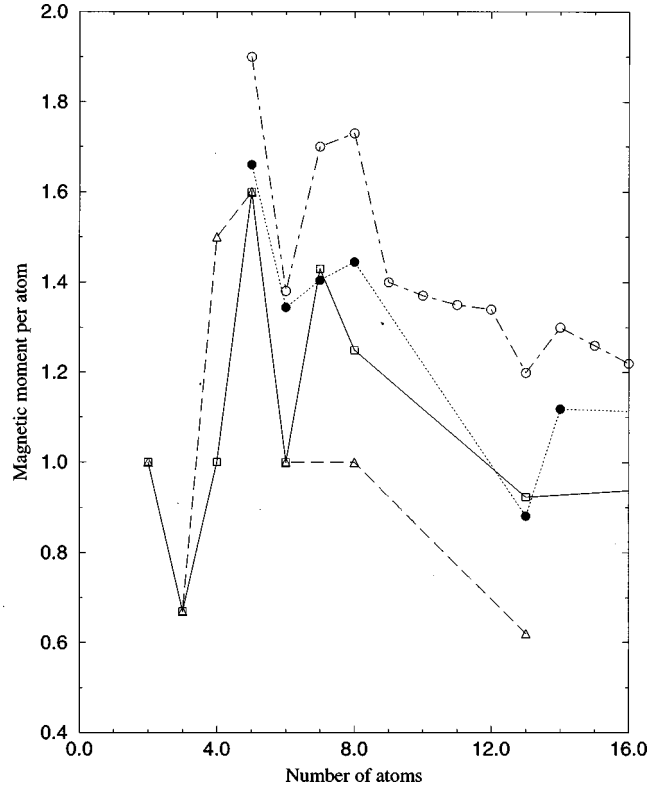

FIG. 1. Theoretical results using the present method (□) and experimental results (Ref. 6) (●) for the average magnetic moments (per atom) of Ni clusters. Results of density-functional-theory calculations in the local-density approximation (LDA) (Ref. 13) are indicated by Δ. Also shown are results of a self-consistent tight-binding method (without full symmetry unconstrained relaxation) reported in Ref. 14 (○).

is more stable than the corresponding icosahedral geometry by 0.131 eV/atom (0.130 eV/atom). It is thus clear that our results for both Ni_{19} and Ni_{43} (being more or less independent of the parametrization used) do not agree with those obtained using the embedded-atom method,[73] according to which Ni_{19} and Ni_{43} exhibit ground states of icosahedral structure.

From these results it is apparent that the current parametrization does not substantially affect the calculated magnetic moments of the clusters (as compared with our results based on our earlier parametrization). In Fig. 1 we plot the average magnetic moment per atom for Ni clusters with $n=2-20$ atoms. We also include in the same figure the experimental results of Apsel *et al.*,[6] the theoretical results of Reuse and Khanna,[13] and the recent theoretical results by Bouarab *et al.*[14] Reuse and Khanna used density-functional theory in the local-density approximation (LDA), while Bouarab *et al.* used a self-consistent tight-binding method (applied to geometries obtained by MD and therefore not fully relaxed within the self-consistent approach) to calculate the average magnetic moments. Our values are in perfect agreement with the LDA results reported in Ref. 13 for $n=2$, 3, 5, and 6. Full optimization can readily be done for clusters of these sizes. As seen in Fig. 1, however, results of Ref. 13 predict a much lower value for the magnetic moment when compared with experiment for Ni_{13}. This may be due to lack of full symmetry and spin unconstrained minimization for this structure. Our results are much closer to experiment than those reported in Ref. 14.

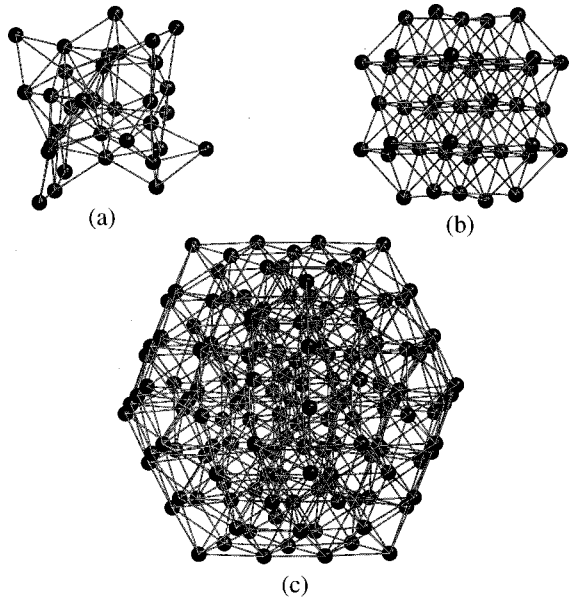

FIG. 2. Relaxed geometries of magnetic Ni_n for $n=$ (a) 33 (twin icosahedron), (b) 43 (fcc), and (c) 147 (icosahedron).

On the other hand, the current parametrization does affect, as expected, the calculated vibrational frequencies of the clusters. For Ni_3 we find the eigenfrequencies to be equal to 98, 183, and 327 cm^{-1}, which are in good agreement with the experimental values of 198, 300, and 405 cm^{-1} as measured by Nour *et al.*[71]

The present method can easily be extended to the treatment of larger Ni clusters. For comparison, we have used our method to study Ni_n clusters for $n=33$ (twin closed icosahedron), 43 (fcc), and 147 (icosahedron) shown in Fig. 2. The magnetic moments for these clusters, along with experimental results for these clusters reported by Apsel *et al.*, are listed in Table V. As seen in the table, there is excellent agreement with experiment for the magnetic moment per atom. The discrepancies, when they arise, have to do with the fact that the experimental results have been obtained at temperatures high enough to account for thermal energies which are comparable with the energy differences among the various isomers of a given cluster. It is also possible that the adsorption of various atoms on the cluster surface tends to promote equilibrium cluster geometries which are different from those exhibited by the adsorption-free magnetic clusters.

TABLE V. Magnetic moment per atom (μ_B) for Ni_n clusters with $n>20$.

		Magnetic moment per atom (μ_B)	
n	Structure	Present work	Expt.[a]
33	twin icosahedron	0.970	0.94
43	fcc	1.070–1.160	1.05
147	icosahedron	0.925	0.85

[a]Reference 6; experimental data have been reexpressed using the gyromagnetic constant $g=2.0$.

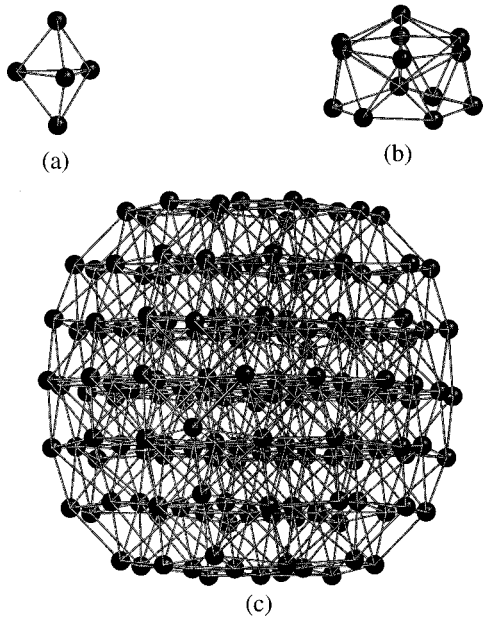

FIG. 3. Relaxed geometries of magnetic Fe_n for $n=$ (a) 5 (trigonal bipyramid), (b) 13 (icosahedron), and (c) 169 (bcc).

B. Fe clusters

As in the case of Ni, the parameters α and ϕ_0 for the Fe_n clusters are obtained by fitting to the ground-state properties of the dimer. In particular, our parameters were fitted so as to reproduce the experimental bond length of 2.02 Å,[74] and the experimental vibrational frequency, $\nu=300\ \mathrm{cm}^{-1}$, (Refs. 71 and 75–77) of the dimer. The parameter s_0, on the other hand, was fitted to reproduce the theoretical spin states of the small clusters.[10,30,31] The values of the parameters a and b were obtained by fitting U_{bond} [given by Eq. (15)] to the experimental value of the cohesive energy of the bulk [4.28 eV/atom (Ref. 72)] and the experimental binding energy of the dimer [0.65 eV/atom (Ref. 75)]. The values of α, ϕ_0, and s_0 (listed in Table II), thus obtained, are slightly different from our previous ones.[30,31] However, the current parametrization does not introduce any quantitative differences in the calculated values of the average magnetic moments $\langle \mu_n \rangle$ for $n<10$, while for larger clusters ($10 \leqslant n \leqslant 55$) the current parameters result in magnetic moments which are at most 6% greater than our previously reported values,[30,31] indicating only a minimal sensitivity of our results to the adjustable parameters. Also, we find no qualitative differences in the ground-state geometries of the clusters studied using the new parametrization. In Table VI, we present our results for some selected Fe_n clusters for comparison. The geometries of some of the relaxed Fe_n clusters are shown in Fig. 3.

As in our previous calculations,[30,31] our results for Fe_n clusters are in very good agreement with both experimental data and theoretical results when the latter pertain to fully relaxed cluster geometries. Thus, we see from our previous results,[30] and from those included in Table VI, that the average magnetic moment $\langle \mu_n \rangle$ per cluster atom exhibits a strong dependence on the cluster size and/or geometry, especially in the case of very small clusters. In Fig. 4 we show the calculated relationship between $\langle \mu_n \rangle$ and the average number of bonds per atom [given by Eq. (16)]. From this it is clear that, as the ratio of surface to bulk atoms becomes smaller, the average magnetic moment tends to stabilize at the corresponding bulk value. For small clusters, however, for which the surface to bulk atoms ratio is larger, a strong dependence of $\langle \mu_n \rangle$ on n_b/n is found, although in this figure it is difficult to separate the effects due to the bond lengths from those due to the average coordination number of the cluster-atoms.

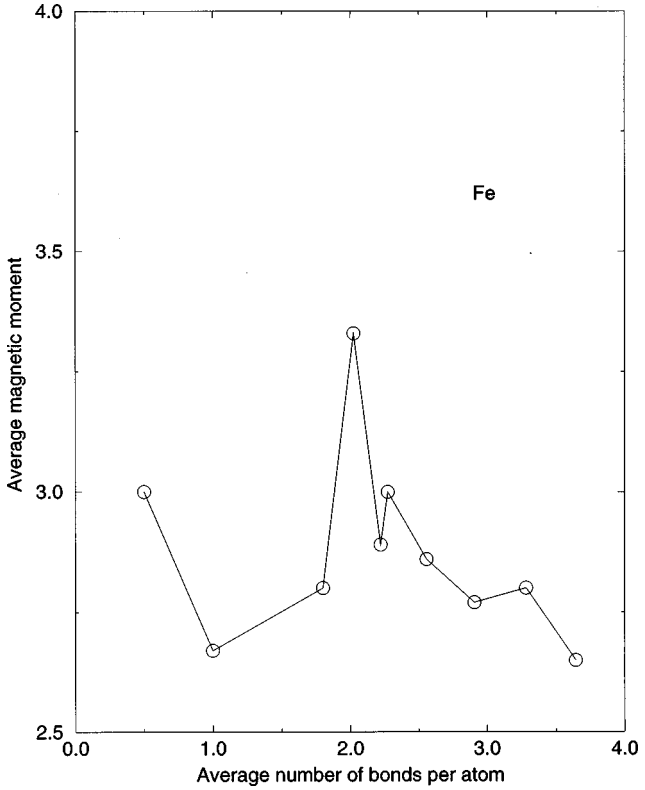

FIG. 4. Average magnetic moment $\langle \mu_n \rangle$ for Fe plotted as a function of the average number of bonds per atom [given by Eq. (16)]. As seen in the figure, the average magnetic moment tends to stabilize at the corresponding bulk value as the ratio of surface to bulk atoms becomes smaller.

The calculated values of $\langle \mu_n \rangle$, in agreement with experiment[5] and other theoretical reports,[10,12,16,20,60] are found to be much larger than those for the bulk ($2.2\mu_B$) (see, for example, Ref. 78). It is worth noting that clusters consisting of hollow structures are found to be stable, in agreement with Christensen and Cohen.[20] These hollow cluster geometries exhibit excessively high magnetic moments. Striking cases appear to be the distorted C_{4v} structure of Fe_6, the cubic Fe_8 and the hollow (no central atom) bcc structure of Fe_{14}. (The hollow icosahedral structure of Fe_{12} (being an icosahedron with no central atom) does not exhibit such property; it is found to be unstable.

Another observation concerning Fe_n clusters is that our results for the magnetic moments of the relaxed cluster geometries are in very good agreement with the results reported by Ballone and Jones[12] and by Pastor, Dorantes-Davila, and Bennemann[16] for relaxed cluster geometries. This indicates that the neglect of the s-d interactions, as noticed in Ref. 16, does not appreciably affect the results, in contrast to the results for Ni_n clusters. At the same time, a comparison between our results and those obtained in Ref. 16 indicates that

TABLE VI. Results for Fe; experimental results have been reexpressed using $g=2.0$.

n	Symmetry	Bonds (Å)	$\langle\mu_n\rangle$ (μ_B)	ω (cm^{-1})	$2s_0$ (eV)	Ref.
2		2.02	3.00	300	2.1	Present
		1.96 (2.00)	3.00		1.7-2.5	26
		1.98	3.00	461		10
		2.04 (2.01) [a]	3.00			12
			3.3 $\pm$0.5			expt. (1)
3	C_{3v}	2.12	2.67	180, 180, 318	2.1	Present
	C_{3v}	2.10	2.67	270, 274, 433		26
	C_{3v}	2.04	2.67			10
	C_{3v}	2.18 (2.14) [a]	2.67			12
			2.7$\pm$0.3			expt. (1)
				180, 220		expt. (71,75,76)
4	Trig. Bip.	2.19$\times$3	3.00	134, 134, 176	2.1	
		2.30$\times$3		184, 184, 308		Present
	Dist. T_d	2.22	3.00	103, 112, 222		
				223, 227, 412		26
	Dist. T_d	2.17,2.43	3.00			12
	Dist. T_d	2.25	3.00			10
5	Sq. Pyram	2.17$\times$4,2.29$\times$4	2.80	68, 100, 117, 144	2.1	
				183, 200, 214, 219, 296		Present
	Trig. Bipyr	2.20$\times$6,2.41$\times$3	2.80	37, 127, 188, 198	2.1	
				213, 296		Present
	Trig. Bipyr	2.22–2.32	2.8–3.2	102, 121, 141, 191		
				205, 256, 270, 323, 401		26
	Trig. Bipyr	2.20$\times$6,2.31$\times$3	2.80			12
	Trig. Bipyr	2.41	3.00		1.46	16
			2.8$\pm$0.2			expt. (26)
6	Tetr. Bipyr	2.32$\times$12	3.33		2.1	Present
	Tetr. Bipyr	2.46	3.00		1.46	16
	Capped Trig. Bipyr	2.16–2.34	3.33			12
7	D_{5v}	2.23$\times$5,2.33$\times$10	2.86			Present
	D_{5v}	2.21$\times$5,2.11$\times$10	3.14			12
	D_{5v}	2.46	3.00		1.46	16
8	Dist. Cube	2.16–2.26	3.00		2.1	Present
9	bcc	2.14	2.89		2.1	Present
	bcc	2.26	2.33		1.46	16
	bcc	2.54	2.89		2.3	17
13	icos	2.23–2.69	2.77		2.1	Present
	fcc	2.54	2.77		2.0	17
	bcc	2.41	2.54		1.46	16
14	bcc (hollow)	2.24	2.86		2.1	Present
15	bcc	2.28	2.80		2.1	Present
	bcc	2.41	2.60		1.46	16
	bcc	2.54	2.93		2.4	17
43	fcc	2.32	2.65		2.1	Present
55	icos	2.3–2.4	2.62		2.1	Present
169	bcc		2.59		2.1	Present

[a]Value obtained by employing a modified spin-polarization function.

significant differences can arise when comparing results obtained for relaxed structures with those obtained for unrelaxed structures. This clearly shows the necessity of performing spin- and symmetry-unconstrained calculations for determining the ground state properties of the CTMA's accurately.

In addition to obtaining the average magnetic moment, our scheme can also provide us with information about the distribution of the magnetic moments and their relationship to the electronic charge transfer among the atoms of the Fe_n clusters. Our calculational results lead to the following conclusions.

(i) The actual value of the magnetic moment $\mu_n^{(i)}$ of the ith atom of a Fe_n cluster is the result of a very delicate interplay of three main factors: (1) the (local) coordination

TABLE VII. Results for Co ; experimental results have been reexpressed using $g=2$.

n	Symmetry	Bonds (Å)	$\langle\mu_n\rangle$ (μ_B)	ω (cm^{-1})	Ref.
2		2.473	2.00	236	Present
3	C_{2v}	2.55,2.69,2.69	2.33	130 132 227	Present
4	T_d	2.61–2.80	2.50	43,78,109,121,132,222	Present
			2.202		25
5	Tetr. Pyr.	2.69×4,2.79×4	2.20	32,81,92,122, 139, 141, 201	Present
6	T_d	2.76	2.33	58,100,113,135,212	Present
			2.332		25
13	hcp	2.71–2.75	2.08		Present
	hcp		2.105		25
	fcc		2.08		80
	icos	2.259 [a]	1.77,2.23		81
	fcc	2.301 [a]	2.08		81
	icos		2.329		25
19	icos	2.54–2.94	2.16		Present
	fcc	2.328 [a]	1.95		81
	fcc	2.508	2.147		25
29	hcp	2.69–2.72	1.90		Present
39	hcp		1.87		Present
43	fcc		1.79		Present
	fcc		2.116		80
43			2.01		expt. (5)
55			1.92		expt. (5)
141			1.82		Present

[a]Optimized bond length only.

number, (2) the bond lengths (between a given atom and its neighbors), and (3) the excess electronic charge $\Delta q_n^{(i)}$ of the given cluster-atom.

(ii) The cluster atoms on the surface exhibit greater magnetic moments than the inner cluster atoms, provided that the corresponding bond lengths and excess electronic charges of the corresponding atoms do not differ appreciably.

(iii) A correlation between $\Delta q_n^{(i)}$ and $\mu_n^{(i)}$ cannot be established, as this is strongly affected by the local coordination number and the bond lengths of the atom with its neighbors.

Thus, for example, in the case of the fcc Fe_{43}, we find that the value of magnetic moment for the central atom is the smallest, while it exhibits a large excess electronic charge of $+0.346$ electrons. The values of the magnetic moments of the rest of the atoms are found to increase as the atoms move away from the central atoms. Atoms belonging to the same shell exhibit the same value of the magnetic moments, and atoms with the highest magnetic moment are found to reside on the outer (surface) shell of the cluster. On the other hand, the excess charges $\Delta q_n^{(i)}$ exhibit a variation with the shell number, the former taking values of -0.256, $+0.035$, and $+0.105$ electrons on the first, second, and third (outer) shells, respectively.

In the case of Fe_{55} we find the excess valence charge $\Delta q_n^{(i)}$ to increase gradually from -0.268 electrons on the central atom to the value of $+0.066$ electrons on the surface atoms. At the same time, the magnetic moments increase from a value of $\mu_n^{(i)}=2.105\mu_B$ (very close to the bulk value) at the central atom to the values $2.68\mu_B$ and $2.78\mu_B$ on the surface and subsurface cluster atoms, respectively, indicating the effect of the interplay of the various factors (discussed above) in the development of the magnetic moment of each cluster atom. This picture is in agreement with the findings of Refs. 16 and 38 in the case of Fe_{15}.

Furthermore, we see from Table VI that our calculations also reproduce the experimental vibrational frequencies of the trimer, Fe_3. In particular, we find $\nu=179.5$ and 318.0 cm^{-1}, which are in good agreement with the experimental values of 180 and 220 cm^{-1} found from far-infrared and resonance Raman spectra.[71,75,76] For larger Fe_n clusters, the frequencies we calculate are included in Table VI along with the results reported by Castro and Salahub[26] for comparison.

Finally, it should be noted that our results are in agreement with the general trends found by Ballone and Jones[12] for small clusters. In particular, we have found that compact clusters are more stable than open structures, and that nonmagnetic clusters exhibit shorter bond lengths than the corresponding magnetic clusters. Additionally, it is worth noting that, while the applicability of the method of Ballone and Jones to Fe_n clusters is limited to cluster sizes $n\leqslant 10$, our method is easily applicable to much larger clusters, and, therefore, offers a significant advantage for studying more complex systems.

C. Co clusters

Unlike in the case of Ni and Fe, the limited availability of the experimental data and *ab initio* results do not permit an accurate evaluation of the adjustable parameters for cobalt at

present. We relied on the data for the bond length and the vibrational frequency of the dimer suggested by Shim and Gingerich[79] (on the basis of their CI calculations) to determine the parameters α and ϕ_0. According to these, the vibrational frequency of Co_2 is approximately 240 cm^{-1}, and the expected bond length is 2.43 Å. To the best of our knowledge, data for small Co_n clusters are very limited. We relied on the existing experimental[3,4] and theoretical data[25,79–81] as well as on our observation (following the studies of Fe and Ni clusters) that the average value of the exchange splitting takes, to a good approximation, the corresponding bulk value, for the determination of the parameter s_0. The parameters a and b were obtained by fitting to the experimental cohesive energy of the bulk [4.39 eV/atom (Ref. 72)] and the experimental binding energy of the dimer [0.5 eV/atom as quoted in Ref. 79. This is very close to the reported theoretical value of 0.482 eV/atom (Ref. 71)]. The adjusted parameters (listed in Table II) reproduce the magnetic ground state of Co_2. This choice of the parameters, however, introduces a small charge transfer between the two Co atoms due to an oscillation in the ground state configuration. Due to the fact that no accurate *ab initio* results are available for Co_2 which can be used for better fitting, we used the parameters listed (in Table II) in our calculations for the larger Co_n clusters in order to demonstrate the applicability of our method.

Our results for the larger Co_n clusters are included in Table VII along with other reported results for comparison. From this table it is apparent that our results reproduce reported results for Co_6 (Ref. 25) and for Co_{13}[25,80] while they decline from the theoretical and experimental results for Co_{43} by 10–15%. On the other hand, our calculations on Co_{141} (Fig. 5) resulting in an average magnetic moment of $1.823\mu_B$, are in very good agreement with the experimental findings of Douglass *et al.*[4] [who found that for cluster sizes of 56–215 atoms the average magnetic moment per atom is $1.96\mu_B \pm 0.12\mu_B$ (re-expressed using gyromagnetic ratio $g=2.0$)] and the experimental results of Billas *et al.*,[5] which indicate a value of $1.75\mu_B$ for cluster sizes of approximately 140 atoms.

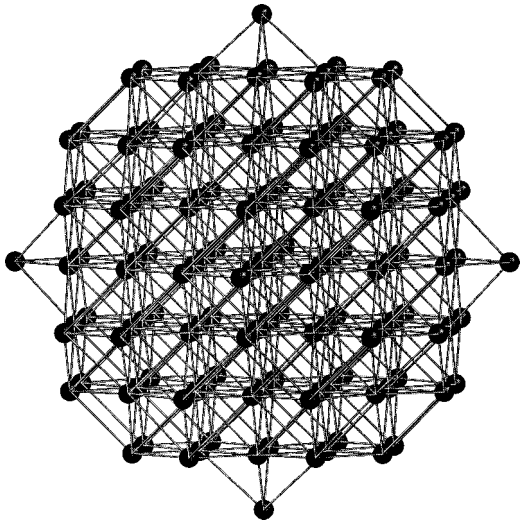

FIG. 5. Relaxed geometry of magnetic 141-atom Co cluster (fcc).

IV. CONCLUSION

We have detailed a minimal parameter tight-binding molecular-dynamics scheme incorporating a Hubbard Hamiltonian for the treatment of magnetic effects. The method is computationally fast, and can be easily used to treat clusters of a few hundred atoms ($n \leqslant 300$). These cluster sizes are well beyond the range of *ab initio* techniques. The present method allows full symmetry and spin-unconstrained minimization for magnetic clusters of size $n > 100$. We have compared our results with experiment and other theoretical schemes. The excellent agreement with experiment for large clusters shows that full geometry optimization is more crucial in obtaining good agreement with experiment than other considerations for magnetic clusters.

ACKNOWLEDGMENTS

We are grateful for useful discussions with J. W. Connolly. The present work was supported by NATO Grant No. CRG 970018, by NSF Grant No. OSR 94-52895, and by the University of Kentucky Center for Computational Sciences.

*Electronic address: super250@convex.uky.edu

[1] D. M. Cox, D. J. Trevor, R. L. Whetten, E. A. Rohlfing, and A. Kaldor, Phys. Rev. B **32**, 7290 (1985).
[2] W. A. de Heer, P. Milani, and A. Chatelain, Phys. Rev. Lett. **65**, 488 (1990).
[3] J. P. Bucher, D. C. Douglas, and L. A. Bloomfield, Phys. Rev. Lett. **66**, 3052 (1991).
[4] D. C. Douglass, A. J. Cox, J. P. Bucher, and L. A. Bloomfield, Phys. Rev. B **47**, 12 874 (1993).
[5] I. M. L. Billas, J. A. Becker, A. Chatelain, and W. A. de Heer, Phys. Rev. Lett. **71**, 4067 (1993); I. M. L. Billas, A. Chatelain, and W. A. de Heer, Science **265**, 1682 (1994).
[6] S. E. Apsel, J. W. Emmert, J. Deng, and L. A. Bloomfield, Phys. Rev. Lett. **76**, 1441 (1996).
[7] A. Maiti and L. M. Falicov, Phys. Rev. B **48**, 13 596 (1993).
[8] C. P. Bean and J. D. Livingston, J. Appl. Phys. Supp. **30**, 120S (1959).
[9] S. N. Khanna and S. Linderoth, Phys. Rev. Lett. **67**, 742 (1991).
[10] J. L. Chen, C. S. Wang, K. A. Jackson, and M. R. Pederson, Phys. Rev. B **44**, 6558 (1991).
[11] P. Mlynarski and D. R. Salahub, J. Chem. Phys. **95**, 6050 (1991).
[12] P. Ballone and R. O. Jones, Chem. Phys. Lett. **233**, 632 (1995).
[13] F. A. Reuse and S. N. Khanna, Chem. Phys. Lett. **234**, 77 (1995).
[14] S. Bouarab, A. Vega, M. J. Lopez, M. P. Iniguez, and J. A. Alonso, Phys. Rev. B **55**, 13 279 (1997).
[15] J. Guevara, F. Parisi, A. M. Llois, and M. Weissmann, Phys. Rev. B **55**, 13 283 (1997).
[16] G. M. Pastor, J. Dorantes-Davila, and K. H. Bennemann, Phys. Rev. B **40**, 7642 (1989); G. M. Pastor, R. Hirsch, and B. Muhlschlegel, *ibid.* **53**, 10 382 (1996).
[17] K. Lee, J. Callaway, and S. Dhar, Phys. Rev. B **30**, 1724 (1984).
[18] K. Lee, J. Callaway, K. Kwong, R. Tang, and A. Ziegler, Phys. Rev. B **31**, 1796 (1985).
[19] B. I. Dunlap, Phys. Rev. A **41**, 5691 (1990); B. I. Dunlap and N.

R. Rosch, J. Chim. Phys. Phys.-Chim. Biol. **86**, 671 (1989).
[20] O. B. Christensen and M. L. Cohen, Phys. Rev. B **47**, 13 643 (1993).
[21] G. M. Pastor, R. Hirsch, and B. Muhlschlegel, Phys. Rev. Lett. **72**, 3879 (1994).
[22] F. A. Reuse, S. N. Khanna, and S. Bernel, Phys. Rev. B **52**, 11 650 (1995).
[23] H. Basch, M. D. Newton, and J. W. Moskowitz, J. Chem. Phys. **73**, 4492 (1980).
[24] M. Tomonari, H. Tatewaki, and T. Nakamura, J. Chem. Phys. **85**, 2875 (1986).
[25] Z-q. Li and B-L. Gu, Phys. Rev. B **47**, 13 611 (1993).
[26] M. Castro and D. R. Salahub, Phys. Rev. B **49**, 11 842 (1994).
[27] M. Menon, J. Connolly, N. N. Lathiotakis, and A. N. Andriotis, Phys. Rev. B **50**, 8903 (1994).
[28] N. Lathiotakis, A. N. Andriotis, M. Menon, and J. Connolly, Europhys. Lett. **29**, 135 (1995).
[29] N. Lathiotakis, A. N. Andriotis, M. Menon, and J. Connolly, J. Chem. Phys. **104**, 992 (1996).
[30] A. N. Andriotis, N. Lathiotakis, and M. Menon, Chem. Phys. Lett. **260**, 15 (1996); Europhys. Lett. **36**, 37 (1996).
[31] A. N. Andriotis, N. Lathiotakis, and M. Menon, in *Proceedings of 1st International Alloy Conference*, edited by A. Gonis, A. Meike, and P. Turchi (Plenum, New York, 1997), p. 261.
[32] N. Rosch, L. Ackermann, and G. Pacchioni, Chem. Phys. Lett. **199**, 275 (1992).
[33] M. Pellarin, B. Baguenard, J. L. Vialle, J. Lerme, M. Broyer, J. Miller, and A. Perez, Chem. Phys. Lett. **217**, 349 (1994).
[34] M. B. Knickelbeim, S. Yang, and S. J. Riley, J. Chem. Phys. **93**, 94 (1990).
[35] H. Kietzmann *et al.*, Phys. Rev. Lett. **77**, 4528 (1996).
[36] E. K. Parks, B. J. Winter, T. D. Klots, and S. J. Riley, J. Chem. Phys. **94**, 1882 (1991).
[37] E. K. Parks, L. Zhu, J. Ho, and S. J. Riley, Z. Phys. C **26**, 41 (1993).
[38] C. Y. Yang, K. H. Johnson, D. R. Salahub, J. Kaspar, and R. P. Messmer, Phys. Rev. B **24**, 5673 (1981).
[39] R. P. Messmer, S. K. Knudson, K. H. Johnson, J. B. Diamond, and C. Y. Yang, Phys. Rev. B **13**, 1396 (1976).
[40] S. Yang and M. B. Knickelbein, J. Chem. Phys. **93**, 1533 (1990).
[41] W. Ekardt, Phys. Rev. B **29**, 1558 (1984).
[42] D. E. Beck, Solid State Commun. **49**, 381 (1984).
[43] J. Lerme, M. Pellarin, B. Baguenard, C. Bordas, J. L. Vialle, and M. Broyer, Phys. Rev. B **50**, 5558 (1994).
[44] J. Lerme, Phys. Rev. B **54**, 14 158 (1996).
[45] D. M. Wood, Phys. Rev. Lett. **46**, 749 (1981).
[46] M. P. J. van Staveren, H. B. Brom, L. J. de Jongh, and Y. Ishii, Phys. Rev. B **35**, 7749 (1987).
[47] A. N. Andriotis, Surf. Sci. **116**, 501 (1982); Phys. Rev. B **32**, 5062 (1985).
[48] C. L. Cleveland and U. Landman, J. Chem. Phys. **94**, 7376 (1991).
[49] S. Valkealahti and M. Manninen, Phys. Rev. B **45**, 9459 (1992).
[50] C. Rey, J. Garcia-Rodeja, and L. J. Gallego, Phys. Rev. B **54**, 2942 (1996).
[51] A. Posada-Amarillas and I. L. Garzon, Phys. Rev. B **54**, 10 362 (1996).
[52] J. Jellinek and E. B. Krissinel, Chem. Phys. Lett. **258**, 283 (1996).
[53] D. A. Papaconstantopoulos, *Handbook of the Band Structure of Elemental Solids* (Plenum, New York, 1986).
[54] F. Liu, M. R. Press, S. N. Khanna, and P. Jena, Phys. Rev. B **39**, 6914 (1989).
[55] R. H. Victora and L. M. Falicov, Phys. Rev. B **31**, 7335 (1985).
[56] G. Fabricius, A. M. Llois, M. Weissmann, and M. A. Khan, Phys. Rev. B **49**, 2121 (1994); **44**, 6870 (1991).
[57] P. Bruno, Phys. Rev. B **39**, 865 (1989).
[58] M. Menon and R. E. Allen, Phys. Rev. B **33**, 7099 (1986); **38**, 6196 (1988).
[59] A. Vega, J. Dorantes-Davila, L. C. Balbas, and G. M. Pastor, Phys. Rev. B **47**, 4742 (1993).
[60] S. Bouarab, A. Vega, J. A. Alonso, and M. P. Iniguez, Phys. Rev. B **54**, 3003 (1996).
[61] X. S. Chen, J. J. Zhao, and G. H. Wang, Z. Phys. D **35**, 149 (1995).
[62] N. Lathiotakis and A. N. Andriotis, Solid State Commun. **87**, 871 (1993).
[63] A. N. Andriotis, J. Phys. Condens. Matter **7**, L61 (1995).
[64] A. N. Andriotis and J. E. Lowther, in *Alloy Phase Stability*, edited by G. M. Stocks and A. Gonis (Kluwer, Dordrecht, 1989), p. 357.
[65] G. Picoli, A. Chomette, and M. Lanno, Phys. Rev. B **30**, 7138 (1984).
[66] W. Harrison, in *Electronic Structure and Properties of Solids* (Freeman, San Francisco, 1980).
[67] J. C. Slater and G. F. Koster, Phys. Rev. **94**, 1498 (1954).
[68] M. J. Mehl and D. A. Papaconstantopoulos, Phys. Rev. B **54**, 4519 (1996).
[69] J. Friedel, in *The Physics of Metals*, edited by J. M. Ziman (Cambridge University Press, Cambridge, 1969), p. 340.
[70] D. Tomanèk and M. A. Schluter, Phys. Rev. B **36**, 1208 (1987).
[71] E. M. Nour, C. Alfaro-Franco, K. A. Gingerich, and J. Laane, J. Chem. Phys. **86**, 4779 (1987).
[72] C. Kittel, in *Introduction to Solid State Physics* (Wiley, New York, 1976).
[73] J. M. Montejano-Carrizales, M. P. Iniguez, J. A. Alonso, and M. J. Lopez, Phys. Rev. B **54**, 5961 (1996); M. S. Stave, D. E. Sanders, T. J. Raeker, and A. E. De Pristo, J. Chem. Phys. **93**, 4413 (1990); T. L. Wetzel and A. E. De Pristo, *ibid.* **105**, 572 (1996).
[74] H. Purdum, P. A. Montano, G. K. Shenoy, and T. Morrison, Phys. Rev. B **25**, 4412 (1982).
[75] M. Moskovits, D. P. DiLella, and W. Limm, J. Chem. Phys. **80**, 628 (1984); M. Moskovits and D. P. DiLella, *ibid.* **73**, 4917 (1980).
[76] D. G. Leopold and W. C. Linenerger, J. Chem. Phys. **85**, 51 (1986).
[77] T. Noro, C. Ballard, M. H. Palmer, and H. Takewaki, J. Chem. Phys. **100**, 452 (1994).
[78] Data from J. S. Smart, *Effective Field Theories of Magnetism* (Saunders, Philadelphia, 1966).
[79] I. Shim and K. A. Gingerich, J. Chem. Phys. **78**, 5693 (1983).
[80] X. Chuanyun, Y. Jinlong, D. Kaiming, and W. Kelin, Phys. Rev. B **55**, 3677 (1997).
[81] K. Miura, H. Kimura, and S. Imanaga, Phys. Rev. B **50**, 10 335 (1994).